# A Terahertz Wireless Communication Link Using a Superheterodyne Approach

Iulia Dan, Guillaume Ducournau, Shintaro Hisatake, Pascal Szriftgiser, Ralf-Peter Braun, and Ingmar Kallfass

*Abstract*—**This paper presents a wireless communication point-to-point link operated in the low terahertz range, at a center frequency of 300 GHz. The link is composed of all-electronic components based on monolithic millimeter wave integrated circuits fabricated in an InGaAs metamorphic high electron mobility transistor technology. Different configurations and architectures are compared and analyzed. The superheterodyne approach proves to be the most promising of all, being compliant with the new IEEE standard for 100 Gbps wireless transmissions and showing compatibility to accessible, already available modems. The first option of realizing the superheterodyne configuration is by combining the 300 GHz transmitter and receiver with of-the-shelf up- and down-converters operating at a center frequency of 10 GHz. In this case, data rates of up to 24 Gbps are achieved. The second option employs a fast arbitrary waveform generator that uses a carrier frequency to up-convert the baseband data. In this case data rates of up to 60 Gbps and transmission distances of up to 10 meters are achieved with complex modulated signals like 16-QAM and 32-QAM. The baseband signal is composed of pseudo-random binary sequences and is analyzed offline using fast analog to digital converters. In superheterodyne configuration multi-channel transmission is demonstrated. Channel data rates of 10.2 Gbps using 64-QAM are achieved. The successful transmission of aggregated channels in this configuration shows the potential of terahertz communication for future high data rate applications.**

*Index Terms*—**Complex modulation, millimeter wave monolithic integrated circuits, multichannel transmission, radio link, terahertz(THz) communications, wireless communication.**

## I. Introduction

Wireless communication technology is one of the fastest growing sectors influencing the society. Our everyday lives and the way we interact on a daily basis with technology drives the need for wireless high data rates. According to [1] this growth is driven by Moore's Law, doubling every 18 months. The prediction for wireless local area network (WLAN) data rates shows that 100 Gbps will already be needed in 2020. Terahertz communication (operating frequencies from 0.1 THz to 10 THz), with its intrinsic high available bandwidth, is a viable solution to provide this high data rate. A recognition of this fact is the new IEEE 802.15.3d standard [2], which allocates the frequency range from 252 to 325 GHz to future wireless communication networks.

One of the most promising applications for terahertz communication represents front- and backhauling. At the moment the connection of access cells to the internet is done by optical fiber. The future exponential growth of individual data rates means that the access cells have to be smaller and appear more frequent. The increasing number of cells will cause additional costs of optical fiber, which is already extremely high in an urban environment. Furthermore, in some remote areas, optical fiber is impossible to use. Therefore, wireless point-to-point high data rate communication operating at frequencies above 200 GHz offers a viable alternative.

There are two options of realizing terahertz communication. The first implies the usage of a very broad bandwidth with a low bandwidth efficiency. For example at a center frequency of 300 GHz, a bandwidth of over 50 GHz is available. Thus, to achieve a data rate of 100 Gbps only 2 b/s/Hz are necessary. The second option implies the usage of aggregated channels each with a small bandwidth and a high bandwidth efficiency.

Up to now mostly the first option has been the focus of research for many groups. Table I shows a summary of high-data-rate wireless links using different technologies. The terahertz signal can be generated either using photonic components like uni-traveling carrier photodiode (UTC-PD) and positive-intrinsic-negative photodiodes (PIN-PD) or active electronics using different technologies either Silicon or III–V compound semiconductor based. [3], [4], [5] and [6] use a combination of a photonic transmitter and an electronic receiver, which is either active or passive, and achieve data rates of 100 Gbps or above. [7] uses an all-electronic approach and an 80 nm InP high electron mobility transistor (HEMT) technology and also achieves 100 Gbps. citeLee2019 and [8] report on Si CMOS integrated transmitters and receivers and on data transmissions using these transceivers. The results are state-of-the-art for this technology with low maximum of oscillation frequencies. In [9] 80 Gbps over a distance of 3 cm are achieved.

Most of the above mentioned publications use a very broadband signal to achieve data rates of around 100 Gbps, hence take advantage of the first option of realizing terahertz communication. The only exceptions are the work presented in [7], in [9] and this work. While [7] and [9] show only measurement results of the high data rate transmission experiment and do not consider the reasons of the architecture choice, this work gives an in-depth analysis of different configurations of a terahertz link presenting advantages and disadvantages of each.

Iulia Dan and Ingmar Kallfass are with the Institute of Robust Power Semiconductor Systems, University of Stuttgart, Stuttgart, Germany e-mail: iulia.dan@ilh.uni-stuttgart.de.

Guillaume Ducournau is with the Institut d'Electronique, Microélectronique et de Nanotechnologies (IEMN), UMR CNRS 8520/Université de Lille, France.

Pascal Szriftgiser is with the Laboratoire de Physique des Lasers Atomes et Molécules (PhLAM), UMR CNRS 8523/Université de Lille, France.

Shintaro Hisatake is with Gifu University, Gifu, Japan.

Ralf Peter Braun is with Deutsche Telekom AG, Berlin, Germany.

TABLE I: State of the art wireless links above 200 GHz using different technologies.

| Ref | Technology | Architecture | Center Frequency | Data Rate | Distance | Modulation Format |
|---|---|---|---|---|---|---|
| [5] | UTC-PD + 35 nm InGaAs mHEMT | zero-IF | 300 GHz | 100 Gbps | 40 m | 16-QAM |
| [3] | UTC-PD + passiv electronic mixer | zero-IF | 280 GHz | 100 Gbps | 50 cm | 16-QAM |
| [4] | UTC-PD + passiv electronic mixer | zero-IF | 425 GHz | 106 Gbps | 50 cm | 16-QAM |
| [10] | 130 -nm SiGe BiCMOS | zero-IF | 230 GHz | 100 Gbps | 1 m | 16-QAM |
| [11] | 130 -nm SiGe BiCMOS | zero-IF | 230 GHz | 90 Gbps | 1 m | 32-QAM |
| [6] | PIN-PD + active electronic receiver | zero-IF | 300 GHz | 128 Gbps | 50 cm | 16-QAM |
| [9] | 40 nm Si-CMOS | superheterodyne | 265 GHz | 80 Gbps | 3 cm | 16-QAM |
| [7] | 80 nm InP-HEMT | superheterodyne | 300 GHz | 100 Gbps | 2.22 m | 16-QAM |
| [12] | 35 nm InGaAs mHEMT | zero-IF | 240 GHz | 96 Gbps | 40 m | 8-PSK |
| [13] | 35 nm InGaAs mHEMT | zero-IF | 240 GHz | 64 Gbps | 850 m | 8-PSK |
| **This work** | **35 nm InGaAs mHEMT** | **superheterodyne** | **300 GHz** | **60 Gbps** | **0.5 m** | **16-QAM** |
| **This work** | **35 nm InGaAs mHEMT** | **superheterodyne** | **300 GHz** | **56 Gbps** | **10 m** | **16-QAM** |
| **This work** | **35 nm InGaAs mHEMT** | **superheterodyne** | **300 GHz** | **12 Gbps** | **0.5 m** | **64-QAM** |

## II. Superheterodyne Approach

The very high data rate transmissions presented above owe their success partly to their transmitters and receivers and accordingly to their high standard technology and partly to the very fast baseband system. All these links involve the usage of fast digital processing equipment both in signal generation, arbitrary waveform generators (AWG) as well as at the receiving end, real-time oscilloscopes. With this kind of equipment pseudo random binary sequences (PRBS) with different lengths can be easily generated, received and post-processed, hence the high data rate.

In order to transmit real-time data and to bring terahertz communications a step closer to real scenario application these costly analog-to-digital and digital-to-analog converters need to be replaced by accessible modems. Thanks to the progress in 5G communication systems, modems based on the IEEE 802.15.3e-2017 [2] and on the ETSI EN 302 217 standard [14] are already commercially available in the V- and E-Band. Combining multiple channels with a narrow bandwidth using complex modulation formats and up-converting them in the 300 GHz band would lead to the full usage of the regions available bandwidth, hence achieving 100 Gbps with real-time data.

This solution implies that the data signal is first up-converted to an intermediate frequency (IF) by the commercially available modems and then up-converted a second time by a 300 GHz transmitter to the H-Band. This translates into a classical superheterodyne architecture, which is very common at lower frequencies, but was never used before for terahertz communication with IF frequencies in the E- and V-Band.

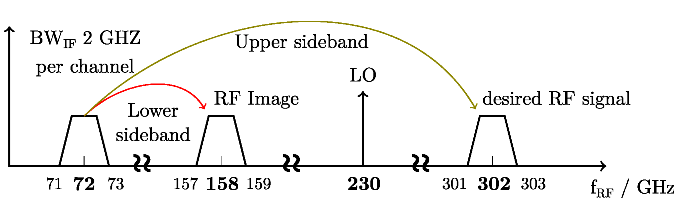


Fig. 1: Frequency spectrum of the IF signal, RF signal and RF image in a superheterodyne system with high IF frequency.

Fig. 1 shows a schematic representation of the superheterodyne approach in terms of frequency spectrum. One modem channel centered around 72 GHz, with a bandwidth of 2 GHz is up-converted using a 300 GHz transmitter with a local oscillator (LO) frequency of 230 GHz. The frequency difference between the desired signal and the image is very high. Thus no complicated filtering needs to be applied.

This paper focuses on the proof-of-concept for the usage of the superheterodyne approach in terahertz communication. Since no RF transmitter and receiver with IF frequencies above 50 GHz are available this work uses a broadband 300 GHz wireless link designed for direct conversion. The link has achieved data rates up to 64 Gbps in zero-IF configuration [15], but was never used in a superheterodyne approach. Although this RF system is not ideal, it serves the purpose of showing that the concept works in the terahertz range.

The superheterodyne architecture is realized by using two different options for the IF component. The first one involves the usage of commercially available mixers, which work as direct up- and down-converters, to generate the IF input and baseband output. The second option is using an IF frequency generated in the AWG. The commercially available mixers have an RF frequency of operation between 7.5 GHz and 20 GHz with an IF frequency range up to 7.5 GHz [16]. Although this range covers the frequency bands X, Ku and K they will be, for simplicity, referred to as X-band mixers. This paper presents a comparison between all these configurations and analyses the advantages and disadvantages of each.

## III. Setup of the Wireless Links

Fig. 2 shows the setup of the wireless communication link in superheterodyne configuration. At the heart of the system presented in this work are the 300 GHz transmitter and receiver based on one monolithic millimeterwave integrated circuit (MMIC) packaged in split-block waveguide modules with a WR-3 output at the RF port and a WR-12 at the local oscillator (LO) input. The MMICs have been described in detail in [17] and are fabricated in a 35nm metamorphic high electron mobility transistor (mHEMT) InGaAs technology [18].

The transmitter consists of a frequency multiplier by three, a buffer amplifier, a fundamental up-converter and a power

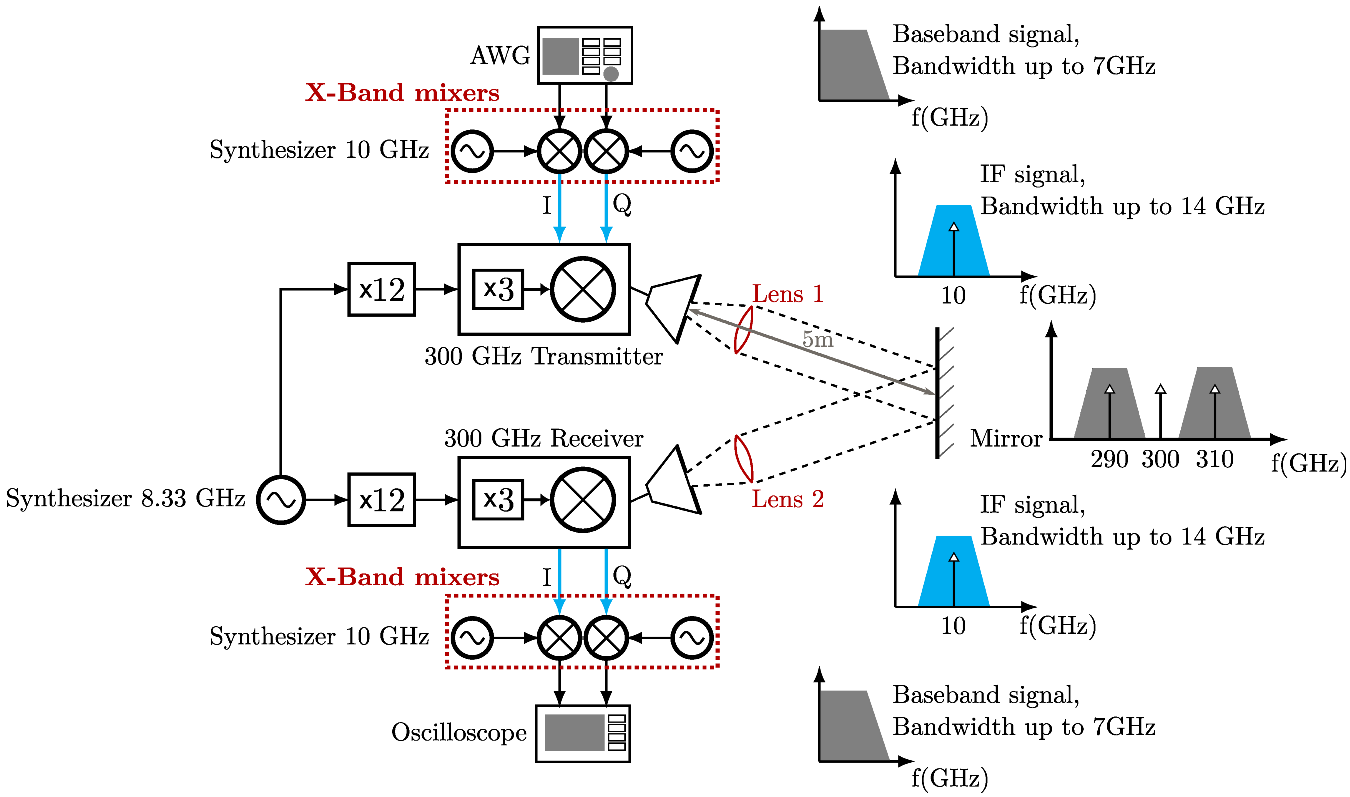


Fig. 2: Setup of the wireless 300 GHz link in superheterodyne configuration with a transmission distance of 10 m. The system is composed of the RF circuitry: the 300 GHz transmitter and receiver including LO generation and the baseband circuitry the X-band mixers, with their respective LO path, for the generation of the intermediate frequency and the digital-to-analog and analog-to-digital converters.

amplifier as a final stage. It achieves a saturated output power of −5 dBm and 20 GHz of IF bandwidth. The receiver integrates a low-noise amplifier, a down-converter and the same LO path as the transmitter. The receiver module achieves an average conversion gain of 6.5 dB, has an RF frequency of operation between 270 and 325 GHz and an average noise figure of 8.6 dB [19].

The 100 GHz LO signal is generated by a separate waveguide multiplier module with a multiplication factor of twelve. The same electrical synthesizer provides the input signal at 8.33 GHz to both transmitter and receiver, thus the setup is coherent. In [20] and [21] it was shown that the white LO noise is the main distortion process for the performance of wireless links operating at frequencies above 200 GHz. Furthermore, it is shown in the above mentioned works that the influence of this impairment is increasing with modulation bandwidth because of the higher amount of accumulated phase error. The noise floor of the signal source used in this work, an Agilent N5183B MXG, is according to the data sheet −112 dBc/Hz measured at 20 kHz offset. The noise floor at the input of the 300 GHz transmitter and receiver is degraded by a factor of $20\log(n)$, where n is the multiplication factor, in this case 12. Therefore, a noise floor of −90 dBc/Hz measured at 20 kHz offset is assumed at the input of the RF components. This calculation is well in accordance to the measurement reported in [22]. This work shows the phase-noise curve of a similar multiplier by twelve module realized using the same technology. The difference between the measured value and the theoretical one, calculated by adding the factor $20\log(n)$ is very small in the range of 2 dB, validating the noise floor value assumed for this work.

The X-Band mixers used to generate the IF signal have an LO of 10 GHz and can cover frequencies of up to 7 GHz at their baseband port. This results in an IF signal centered around 10 GHz with a bandwidth of up to 14 GHz, like represented in Fig. 2 in the IF spectrum in blue. The in-phase and quadrature (I/Q) data signal is generated by an Arbitrary Waveform Generator (AWG) using Pseudo Random Binary Sequences (PRBS) with a length of $2^{15}-1$. On the receiver side a real time oscilloscope captures the I- and Q-signals from the receiving X-band mixers. The incoming signal is analyzed and post-processed by a vector signal analyzer software, which performs the carrier recovery and frequency equalization to compensate for the frequency and phase drift along the link. The digital equalization tool of the software has been applied to all the results shown in this paper.

The figure of merit for the performance of the link chosen for this work is the measured root mean square error vector magnitude (EVM). The advantages of EVM are that it can be easily obtained from most available measurement devices, it represents a requirement for most wireless standards and, in comparison to bit error rate (BER), it provides information about the source of impairment that occurs in the system. Amplitude and phase imbalances, DC offset, phase noise have a particular signature in the constellation diagram and are reflected in the measured EVM [23]. A transmission is considered successful when the probability of a bit error is smaller than $4 \cdot 10^{-3}$, which can be reduced to $10^{-15}$ using forward error correction codes [24]. The probability of error, $P_\mathrm{b}$ is dependent on the ratio of bit energy to noise power density, $E_\mathrm{b}/\mathrm{n}_0$, where $E_\mathrm{b}$ is the energy received during each bit interval, and $n_0$ is the power spectral density of the noise on the channel following the dependency

$$P_\mathrm{b} = \frac{1}{2}\mathrm{erfc}\left(\sqrt{\frac{E_\mathrm{b}}{n_0}}\right). \tag{1}$$

Hence, a certain $E_\mathrm{b}/\mathrm{n}_0$ can be associated to a BER of $4 \cdot 10^{-3}$, considering coherent demodulation and an Additive White Gaussian Noise (AWGN) channel. $E_\mathrm{b}/\mathrm{n}_0$ can be converted to the signal to noise ratio (SNR) by

$$E_\mathrm{b}/\mathrm{n}_0 = \mathrm{SNR} - k_{\mathrm{roll-off,mod}}, \tag{2}$$

where $k_{\mathrm{roll-off,mod}}$ is a correction factor that takes into account the used modulation format and digital filter [25], [26]. SNR is, like the EVM, obtained from the measurement devices. Table II shows the EVM limits for successful transmissions when all of the above considerations are made.

TABLE II: Limits for successful transmissions based on measured SNR and theoretical $E_\mathrm{b}/\mathrm{n}_0$.

| Modulation format | $k_{\mathrm{roll-off,mod}}$ | SNR in dB | EVM in % |
|---|---|---|---|
| QPSK | 3.01 | 11.5 | 26.5 |
| 16-QAM | 6.02 | 16.9 | 15.2 |
| 64-QAM | 7.78 | 23.3 | 6.8 |

Two different antenna systems are used depending on the desired transmission distance. A first experiment with two horn antennas with 22 dBi gain are used to cover 50 cm. The second systems uses two horn antennas with 25 dBi gain and two 100 mm teflon lenses leading to a total estimated gain of around 38 dBi on each side, which are used to transmit the signal over a distance of 10 m. The transmission is obtained with a reflection on a mirror placed at 5 m distance from the emission/detection modules.

## IV. Short Range Wireless Data Transmission

For the first data transmissions a distance of half a meter is chosen between the transmitter and the receiver. To have more control over the RF input power at the receiver a waveguide variable attenuator is placed between horn antenna and receiver module. To determine its optimal power a sensitivity analysis needs to be carried out. For this purpose the AWG and the oscilloscope are connected directly to the IF ports of the transmitter and receiver. The RF input power is varied with the help of the variable attenuator and different modulation formats and symbol rates are transmitted. The transmission is evaluated in terms of error vector magnitude (EVM), measured in % and plotted versus the input power. The power at the output of the attenuator, which corresponds to the input power at the receiver, is measured with a powermeter.

Fig. 3 shows the receiver's sensitivity dependency on the used modulation format. The symbol rate is kept constant at 1 GBd. The more complex the modulation format, the lower the threshold in % for a successful transmission.

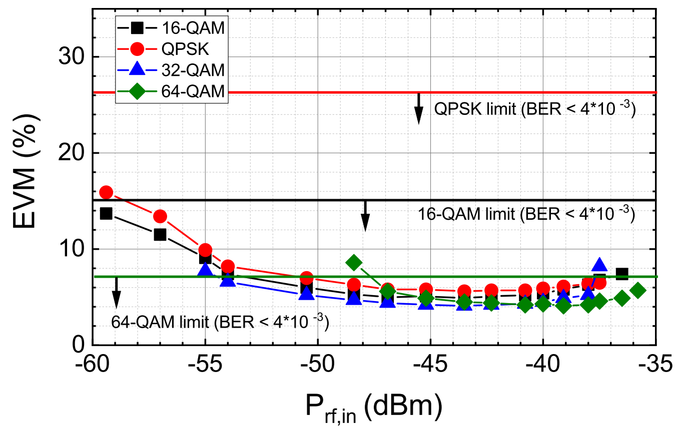


Fig. 3: Sensitivity curves of the 300 GHz receiver for different modulation formats and signals with a symbol rate of 1 GBd.

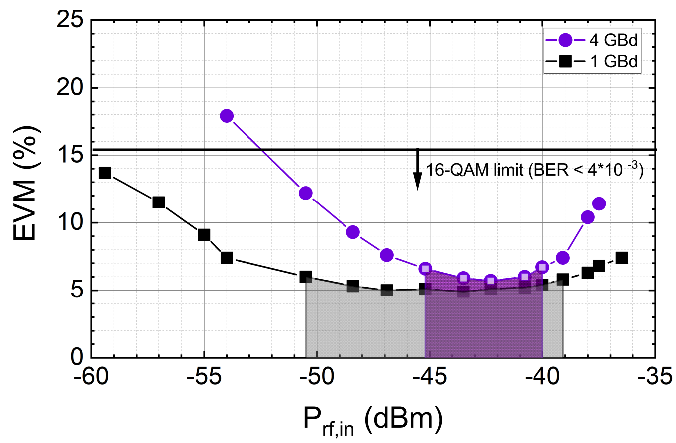


Fig. 4: Sensitivity curves of the 300 GHz receiver for increasing symbol rates for 16-QAM modulation format.

For 1 GBd symbol rate and for the modulation formats 16-QAM and 32-QAM the region with minimal EVM stretches over a wide range of input power, from around −38 to over −50 dBm. For the more complex modulation format of 64-QAM represented in the green line with diamond symbols the range of optimal input power is narrower going only up to −45 dBm. As a conclusion, the optimal input power range for all used modulation formats lies between −38 and −45 dBm, for a symbol rate of 1 GBd.

The sensitivity curve is not only dependent on the modulation format but also on the data rate. Fig. 4 shows this dependency for two symbol rates1 GBd and 4 GBd and 16-QAM modulation format. The probability of error is proportional to the data rate, which explains why the EVM value increases as the symbol rate increases. In addition, it can be observed in Fig. 4 that the optimal input power range decreases with increasing symbol rate. The marked area below the curves, where the EVM is at its minimum ranges for the 4 GBd signal from −40 to over −45 dBm.

An input power of around −40 dBm seems to be the best compromise for all modulation formats and low and high

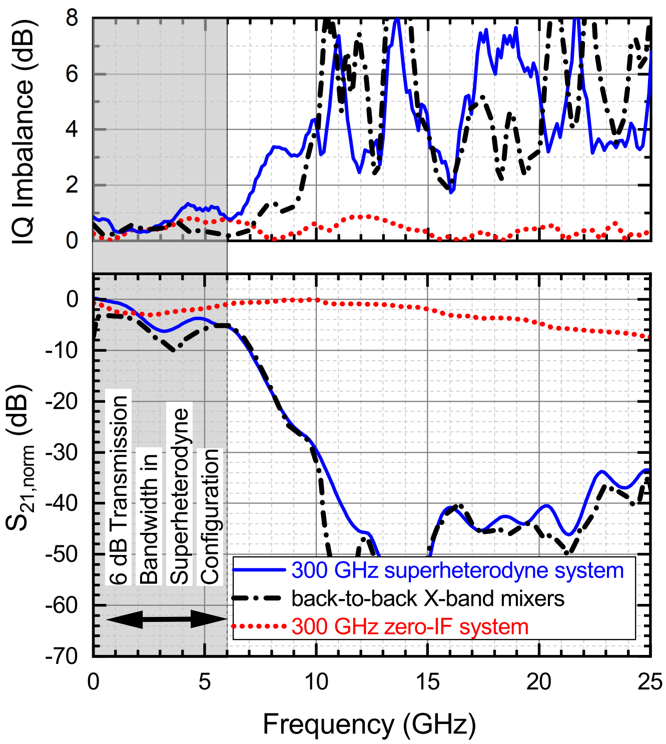


Fig. 5: Transfer function and amplitude imbalances of the transmission system for different scenarios: in black dash-dot line the back-to-back measurement of the X-band mixers, in red dotted line the zero-IF 300 GHz system and in blue solid line the superheterodyne 300 GHz system, when the IF is provided by the X-band mixers.

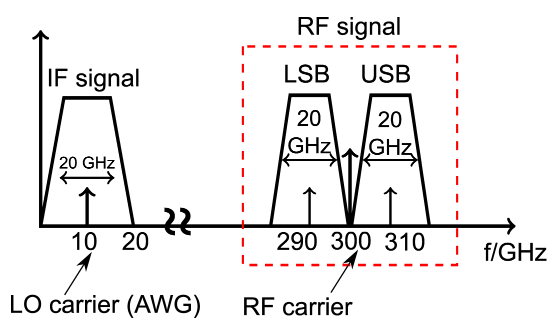


Fig. 6: Spectrum of the RF signal for a superheterodyne link realized using an IF generated in the AWG, centered around 10 GHz. The highest possible transmission bandwidth is 20 GHz, which allows no overlap between LSB and the USB.

symbol rates. The optimum setup of the RF receiving power is the prerequisite for the best possible transmission results.

The next step in the correct analysis of transmission results is the measurement of the transfer characteristic for the overall wireless link. Initially, the response of the transmitted signal through the X-band mixers is measured. For this purpose, the four X-band mixers are connected in a back-to-back configuration, the I X-band transmitter mixer is directly connected to the I-receiver mixer and the same applies for the Q path. A network analyzer is used to measure the scattering parameters from the transmitter to the receiver. The $S_{21}$ parameter is then normalized to its maximum value and plotted versus the frequency. In Fig. 5, the black dash-dot line shows the results of this measurement. The 6 dB IF bandwidth is around 7 GHz, which corresponds well to the IF bandwidth mentioned in the data sheets of 7.5 GHz [16]. The difference between the transmission on the I-channels and on the Q-channels represents the IQ amplitude imbalance of the system which is plotted on the upper y-axis. The value of the imbalance remains below 1 dB for the IF bandwidth of the transmission and increases considerably after the upper frequency of 7 GHz.

In Fig. 5, the red dotted line represents the transfer characteristic of the 300 GHz transmit-receive system, when the baseband signal is generated directly in the AWG with no frequency offset. The zero-IF system has a 6 dB bandwidth of 20 GHz, with an IQ amplitude imbalance of below 1 dB over the IF bandwidth. Therefore, it is well suited to validate the proof of concept for the superheterodyne system. According to this transfer characteristic the best choice for the intermediate frequency is around 10 GHz, which represents the best compromise between low imbalances, good transfer behavior between transmitter and receiver and achievable data rates using the X-band mixers. Another reason why 10 GHz is a suitable IF frequency is the spacing between the lower side band (LSB) and upper side band (USB). A higher IF frequency would lead to a higher available gap between LSB and USB reducing the risk of overlapping, but it would come at the cost of smaller available bandwidth in the superheterodyne system. For example, an IF signal centered around 15 GHz with a bandwidth of 20 GHz would have a corner frequency of the USB at 325 GHz. Like previously mentioned, the 6 dB bandwidth of the zero-IF transmission lies slightly above 20 GHz. This translates into an RF signal with an upper corner frequency of around 320 GHz. Hence, the transmission of the above mentioned IF signal would not be possible in a superheterodyne system.

The transfer characteristic of the final superheterodyne system as pictured in Fig. 2 is presented in Fig. 5 by the blue solid line. These results correspond well with the measurement of the X-band mixers in back-to-back configuration. The IF bandwidth is the same as in the case of the dash-dot line, 8 GHz. Also the two characteristics follow similar curves, therefore the system is limited by the X-band mixers.

Data transmission experiments using different modulation formats and symbol rates have been carried out and the quality of the transmission has been analyzed. Fig. 7 summarizes the results for 16-QAM and 32-QAM modulation formats and symbol rates up to 15 GBd. The used digital filter was raised cosine with a roll-off factor of 0.35 and it was kept constant for all transmissions.

Fig. 7 shows the performance comparison of different configuration of the wireless link for two modulation formats: 16-QAM and 32-QAM. First back-to-back transmissions from the AWG to the oscilloscope were made. These represent the reference measurement of the used equipment and are plotted in all three graphs using the pink line with pentagon symbols. Another reference measurement in back-to-back configuration is the one of the X-band mixers, which is represented with the

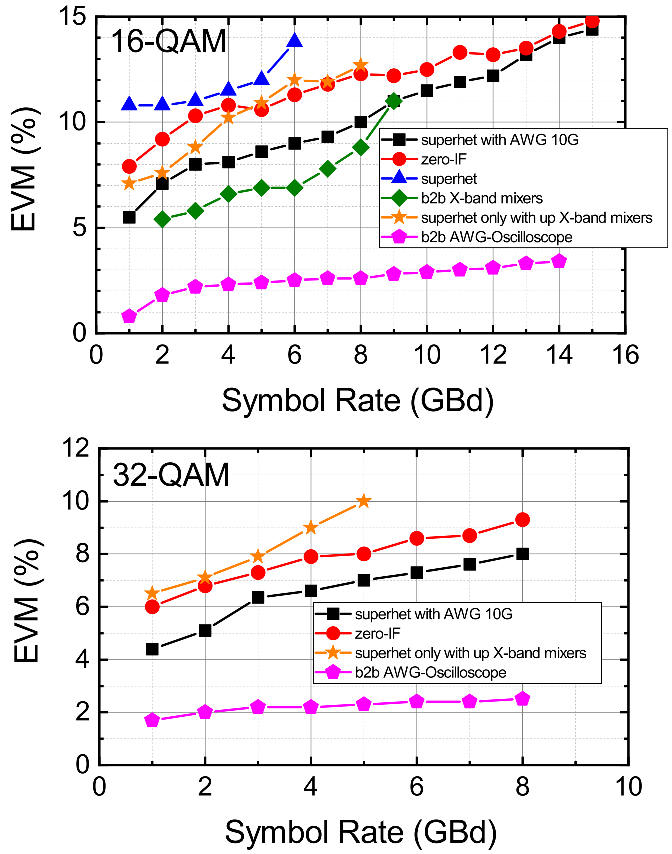


Fig. 7: Results of the 300 GHz wireless data transmission realized using different architectures for increasing symbol rates. Two modulation formats are analyzed: 16-QAM and 32-QAM. All the transmissions show an EVM which is below the BER threshold smaller than $4 \cdot 10^{-3}$, calculated for a AWGN channel.

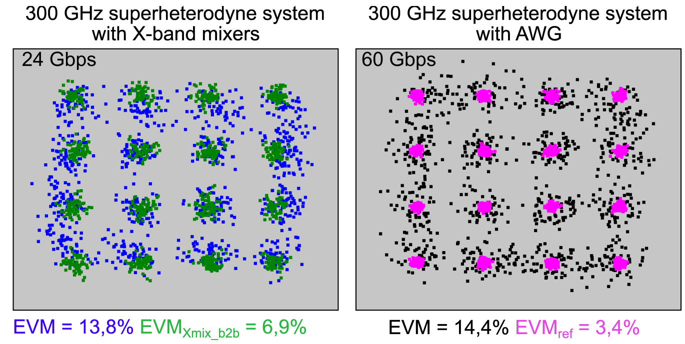


Fig. 8: Constellation diagrams for 16-QAM modulated signals achieved using the 300 GHz superheterodyne system. For the transmission plotted on the left external mixers were used and for the transmission on the right the AWG provides the IF signal.

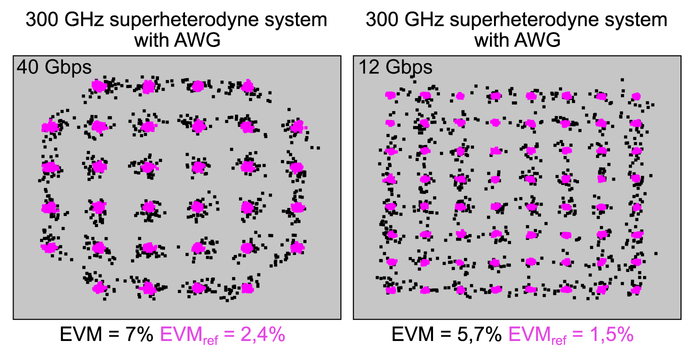


Fig. 9: Constellation diagrams for higher order modulated signals achieved using the 300 GHz superheterodyne system with the AWG.

green line with diamond symbols. For the 300 GHz link four scenarios are considered. The first uses a zero-IF approach and is plotted using the red line with round symbols. The last three scenarios use a superheterodyne approach under different conditions. The black line with the square symbols shows the results when the AWG is generating the data centered around an IF frequency of 10 GHz. In this case the oscilloscope and the post-processing software down-convert the IF signal to the baseband. The orange line with the star symbols shows the results of transmission where the baseband signal generated in the AWG is up-converted to an IF frequency by the X-band mixers. The down-conversion to baseband is done by the oscilloscope and the post-processing software like in the previous case. The last case represents the superheterodyne transmission using X-band mixers both on transmitter and receiver side and is plotted in the blue line with triangle symbols.

For all scenarios the EVM is degrading with increasing symbol rate due to the bandwidth limitations presented in Fig. 5. Besides the two reference measurements, the equipment calibration and the back-to-back transmission of the X-band mixers, the best performance is achieved using the superheterodyne architecture when the IF is generated in the AWG. For 16-QAM modulation a symbol rate of 15 GBd corresponding to a data rate of 60 Gbps and to a bandwidth of around 20 GHz is reached. On the one hand, this is the maximum achievable data rate due to the bandwidth limitations of the 300 GHz link. Fig. 5 shows that the zero-IF system represented with the red dotted curve has a 6 dB bandwidth of around 20 GHz. On the other hand, the analog bandwidth of the measurement equipment is also 20 GHz. In addition, this bandwidth of 20 GHz is the limit for a transmission without an overlap between LSB and USB. Fig. 8 shows the constellation diagrams of the highest data rate achieved with the two superheterodyne systems. For the transmission plotted on the left external mixers were used and a maximum data rate of 24 Gbps is achieved. The bandwidth occupied by the 6 GBd signal achieving this maximum data rate corresponds to the 6 dB bandwidth measured and plotted in Fig. 5. For the transmission plotted on the right, the AWG is used to generate the IF signal. In this case a maximum data rate of 60 Gbps can be achieved.

Another important aspect of terahertz wireless links is the possibility of transmitting higher order modulation formats. The bottom graph in Fig. 7 shows the results for 32-QAM modulation. The 300 GHz RF components exhibit a high linearity, so that the transmission of 32-QAM modulated signals

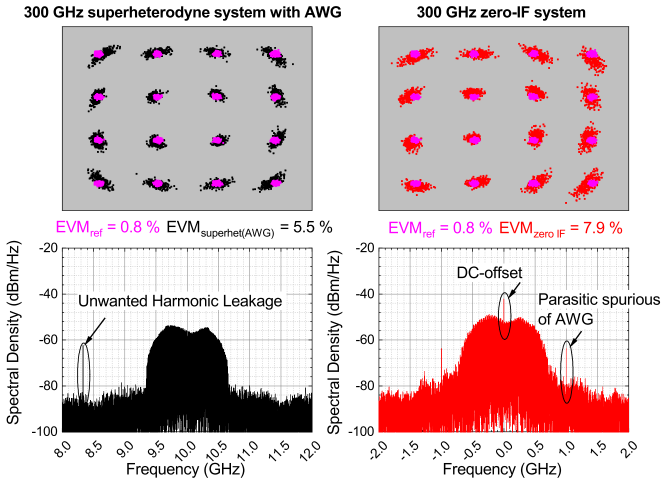


Fig. 10: Constellation diagrams and power spectras for a 16-QAM signal with a symbol rate of 1 GBd using zero-IF configuration (right) and a superheterodyne configuration, where the superheterodyne has been realized using an AWG (left).

is possible. This is presented in the red curve which shows the results of the zero-IF transmission. The X-band mixers on the other hand do not have the necessary linearity for complex modulated signals. The reference measurement of these mixers shows that 32-QAM transmission is not successful. The green line with diamond symbols is absent in Fig. 7 in the lower graph. The limiting factor is represented by the down-converter X-band mixers as the transmission with external mixers on the transmitter side is successful up to a symbol rate of 5 GBd as presented in Fig. 7 in the bottom graph by the yellow line with star symbols.

Due to the high linearity of the RF transmitter and receiver a successful transmission of 32-QAM modulated signal is realized using the superheterodyne link which uses the AWG to generate the IF signal. Fig. 9 shows the constellation diagrams for the highest data rates achieved in this configuration. For 32-QAM modulation 40 Gbps are reached. 64-QAM modulation was successful up to a data rate of 12 Gbps.

To have an in depth analyis of the performance of the superheterodyne link two important comparisons need to be discussed. The first one is the comparison between the zero-IF and the superheterodyne approach using the AWG as IF generator, in the graphical representation the comparison between the red line with round symbols and the black line with square symbols. The superheterodyne approach shows better results than the zero-IF one for all modulation formats. To better visualize the reasons for this difference Fig. 10 shows the constellation diagrams and power spectra for a 16-QAM signal with a symbol rate of 1 GBd using the above mentioned approaches. For a better understanding of the transmission deterioration, in the constellation diagrams the results of the reference measurement were plotted in pink.

The transmission using the zero-IF approach is more erroneous because of impairments like DC-offset and parasitic spurious caused by the AWG at the symbol rate value, in the case pictured in Fig. 10 right at 1 GHz. In addition, at zero-IF the LO frequency locking is harder to achieve. A visible impairment in the superheterodyne transmission presented in Fig. 10 on the left is the leakage of an unwanted mixing product at 8.33 GHz. Another important reason for a better performance of the superheterodyne approach is the flatter frequency response of the overall system presented in Fig. 5 in the dotted red line. Given the bandwidth of 1.35 GHz of this case, the ripple of the $S_{21}$ parameter for signal with a center frequency of 10 GHz is smaller than 0.3 dB. For a signal centered around DC the same ripple exceeds 1.5 dB.

With increasing symbol rates the EVM difference between the zero-IF and the superheterodyne approach becomes smaller. This is caused by the surpass of the 3-dB bandwidth of the system. If we consider a signal centered around 10 GHz with a bandwidth of 13.5 GHz, the upper frequency of 16.75 GHz is above the 3-dB bandwidth limit, which lies at 16 GHz. For 32-QAM only symbol rates of up to 8 GBd lead to successful transmissions and the difference between zero-IF and superheterodyne approach remains approximately constant.

The second important comparison is the one between different superheterodyne scenarios. In this case the reference measurement is, next to the one of the equipment AWG-Oscilloscope, the measurement of the X-band mixers in back-to-back configuration. Due to the bandwidth limitation of the commercial mixers only symbol rates of up to 9 GBd can be transmitted using 16-QAM modulation [16]. For 32-QAM no successful transmission was achieved. To determine why, transmissions with X-band mixers only on the transmitter side are conducted. The fact that these transmissions were possible up to a symbol rate of 5 GBd shows that impairments of the X-band down-converters represent the limitation factor for the back-to-back X-band mixers transmission in the case of 32-QAM modulation.

For 16-QAM modulated signals the difference between the superheterodyne system in blue and the reference measurement in green is around 5 %. The degradation is due to the influences of the 300 GHz transmitter and receiver and their impairments: IQ amplitude and phase imbalances and leakage of unwanted spurious tones.

Fig. 11 shows the comparison of transmission results of the 300 GHz superheterodyne link in different configurations: in blue, in the middle, the superheterodyne link using the X-band mixers and in orange, on the right superheterodyne link using X-band mixers only on the transmitter side. In addition the measurements of the reference signal of the X-band mixers in back-to-back configuration are plotted in green on the left. For this comparison a 16-QAM signal with a symbol rate of 4 GBd was transmitted. In all three cases the results of the back-to-back transmission from AWG to Oscilloscope has been additionally plotted in the constellation diagram.

A strong interference and degradation cause represents the LO leakage of the X-band down-converters. The signal at 10 GHz is present in the green and in the blue curve, but not in the orange one. The leakage of second harmonic of the X-band up-convert LO can be observed at 20 GHz in the left graph. In addition other undesired spurious tones resulting from the

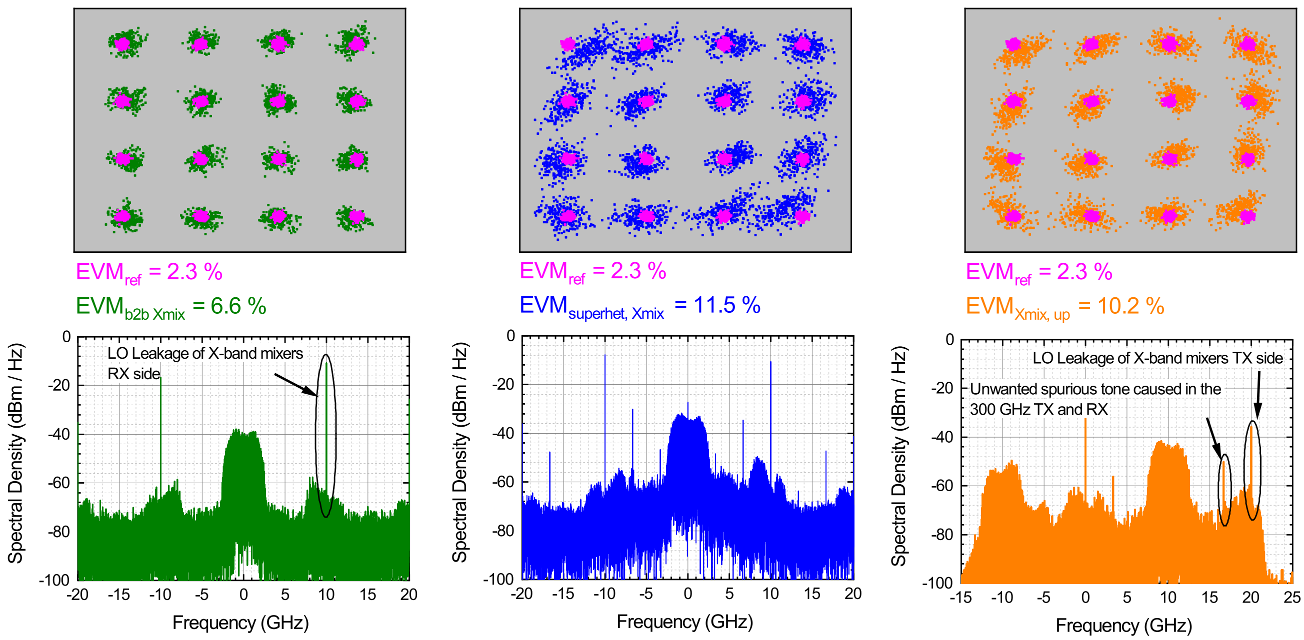


Fig. 11: Constellation diagrams and power spectras for a signal with a symbol rate of 4 GBd, modulated with 16-QAM using the X-band mixer link in back-to-back configuration (left), a superheterodyne configuration, where the superheterodyne architecture has been realized using the X band mixers (center) and a superheterodyne configuration, where the superheterodyne architecture has been realized using the the X band mixers only on the transmitter side (right).

mixing in the 300 GHz transmitter and receiver corrupt the signal and degrade the EVM for the superheterodyne link in blue. The fact that the orange spectrum on the right presents only one spurious tone at 16.66 GHz shows that the X-band down-converters are the limiting factor of the transmission.

Despite the fact that the X-band mixers are not designed for terahertz communication application and do not meet the requirements necessary for transmitting data rates in the range of 100 Gbps, data transmissions using the superheterodyne concept were successful up to a data rate of 24 Gbps. Another impediment is that the used 300 GHz transmit-receive system was designed mainly for zero-IF configuration. Considering this, the maximum data rate of 60 Gbps achieved with the AWG shows the potential of this concept.

## V. 10 Meter Wireless Transmission

To validate the concept also for longer distances and prove its suitability for future indoor wireless applications data transmissions over a distance of 10 m are conducted. The superheterodyne architecture is realized for these transmissions with the AWG, which generated the IF signal centered around a carrier of 10 GHz.

Prior to the 10 m experiment, measurements in back-to-back configuration with a variable attenuator placed between the 300 GHz transmitter and receiver are conducted. As in the case of the longer distance transmission the superheterodyne concept is realized using the AWG and an IF centered around 10 GHz. The variable attenuator is set for an optimal RF input power of −40 dBm into the receiver. The same input power reaches the receiver also in the other two transmission cases: 0.5 m and 10 m.

Data transmissions using signals modulated with QPSK, 16-QAM and 32-QAM are conducted and compared to the 0.5 m low distance transmission as well as to the back-to-back configuration. Fig. 12 shows the results of this comparison. The three transmissions show very similar performances, which was expected due to same RF input power at the receiver. The highest data rate of 56 Gbps is achieved for the transmission distance of 10 m with 16-QAM. Successful transmissions were realized also with more complex modulation formats like 32-QAM. For this case the highest data rate achieved is 30 Gbps.

The successful 10 m experiment shows that additional free space path loss can be easily compensated by an antenna system with enough gain and therefore the superheterodyne architecture is a promising concept for future indoor and outdoor wireless links.

## VI. Multichannel Transmission

The potential of the superheterodyne concept unfolds under multichannel transmission, also called channel aggregation. The new IEEE standard for 100 Gbps wireless point-to-point links [2] defines channels with a bandwidth of 2.16 GHz to be aggregated in the low THz range between 252 and 325 GHz. Based on this standard, multichannel transmissions using the system presented in Fig. 2 were conducted. The signals were generated with the help of the AWG. For this experiment two channels were aggregated, each with a bandwidth of 2.16 GHz. Different modulation formats and digital filters were applied.

Fig. 13 shows the constellation diagrams and power spectrum of an 32-QAM modulated IF signal. The two center frequencies of the channels at 10 and 12.16 GHz are close to the center frequency of the single carrier experiments. A

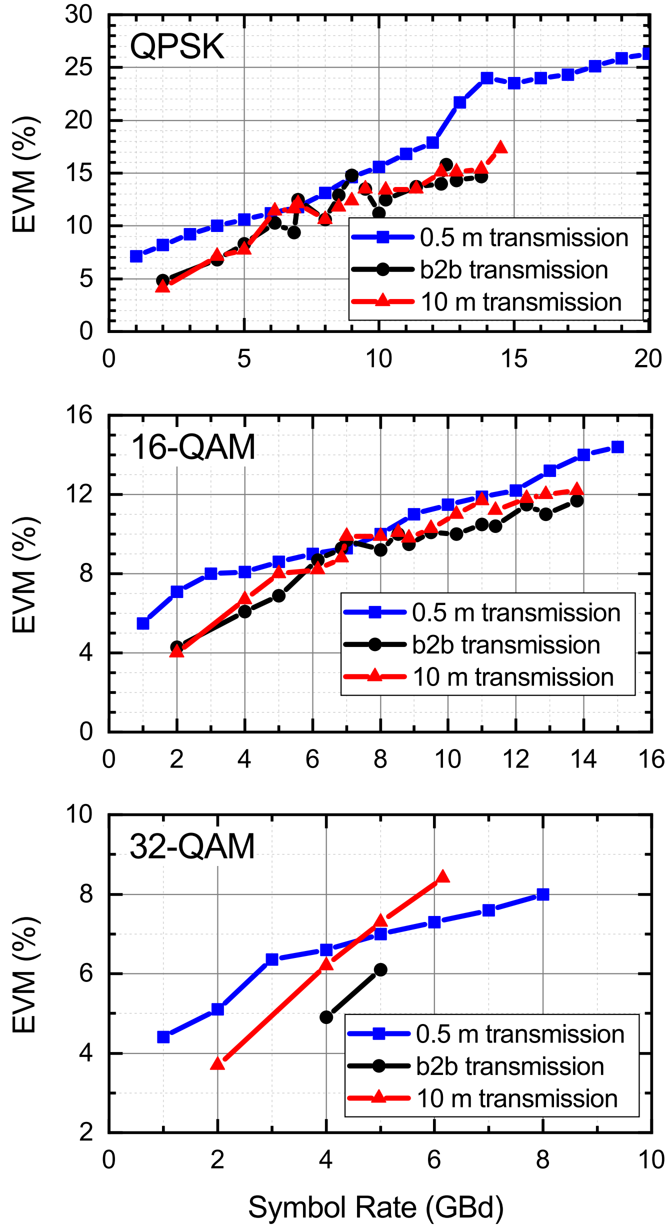


Fig. 12: Comparison of 300 GHz wireless data transmission results over different distances. Three modulation formats are analyzed: QPSK, 16-QAM and 32-QAM.

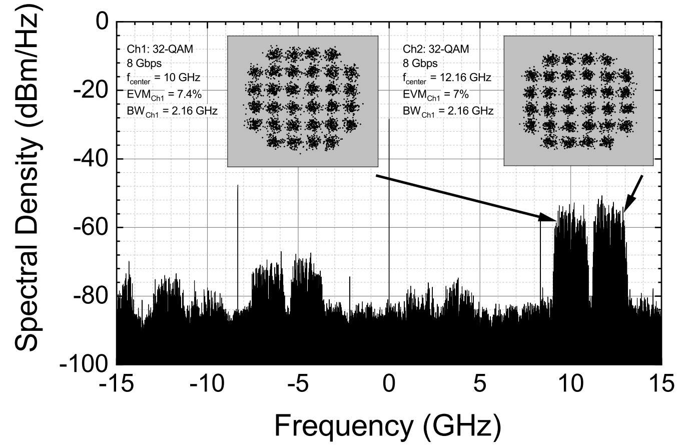


Fig. 13: Successful transmission of a multi carrier 32-QAM modulated signal in a superheterodyne 300 GHz wireless link. On each channel a data rate of 9.6 Gbps and an overall aggregated data rate of 19.2 Gbps is achieved.

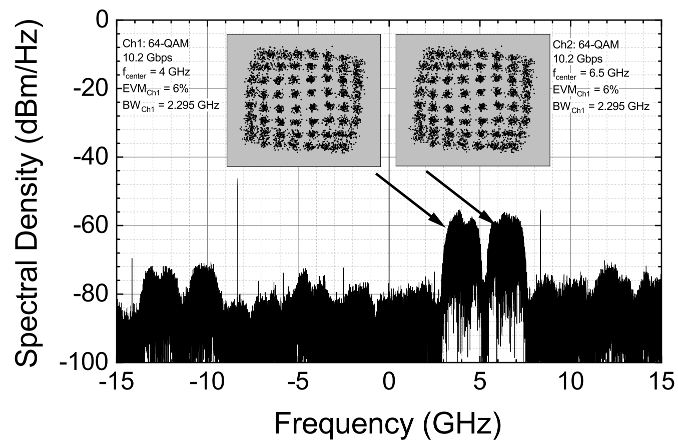


Fig. 14: Successful transmission of a multi carrier 64-QAM modulated signal in a superheterodyne 300 GHz wireless link. On each channel a data rate of 10.2 Gbps and an overall aggregated data rate of 20.4 Gbps is achieved.

channel data rate of 8 Gbps is achieved. The performance of the second channel, centered around 12.16 GHz is slightly better than that of the first channel, the EVM value reaches 7 % in comparison to 7.4 % on the first channel. Compared to the experiment presented in Fig. 7, the performance of the transmission has deteriorated. The EVM increases from around 4.2 % to 7.4 %. This deterioration is caused by the interference with the second channel.

Fig. 14 shows the constellation diagrams and power spectrum of an IF signal, that achieved the highest channel data rate. The chosen modulation format is 64-QAM, the symbol rate is 1.7 GBd and the digital filter has a roll-off factor of 0.35, which leads to a bandwidth of 2.295 GHz. The first channel is centered around 4 GHz and the second one is centered around 6.5 GHz. The data rate transmitted on each channel reaches 10.2 Gbps. The two channels perform similar, they both have an EVM of 6 %.

The focus of the multichannel transmission was the compatibility to the new IEEE standard, which foresees channel bandwidths of around 2 GHz. A comparison to the single carrier experiment shows the impact of channel aggregation on the linearity of the system. Fig. 9 shows that a data rate of 12 Gbps can be achieved with 64-QAM modulation when only one channel is transmitted. In the multichannel experiment this data rate is reduced to 10.2 Gbps due to a higher peak to average power ratio. To achieve the same data rate as in the single carrier transmission a higher back-off from the 1 dB point is required. This, however, leads to a lower SNR. Therefore, it can be stated, that a high linearity of the transceiver is one of the crucial issues for this type of transmission.

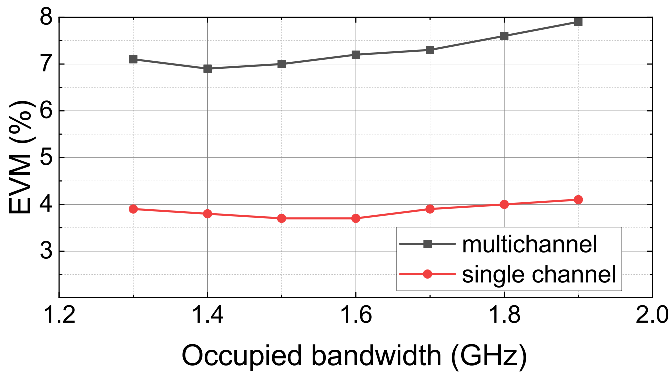


Fig. 15: Performance comparison between single channel and multi channel transmission for a QPSK modulated signal with a symbol rate of 1 GBd and an increasing roll-off factor of the filter.

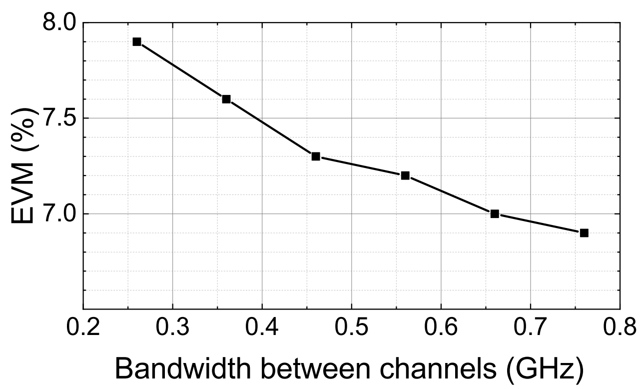


Fig. 16: Deterioration of wireless link performance due to interferences in a multichannel transmission.

Fig. 15 shows the influence of a multi-carrier signal on the performance of the link. For this measurement the transmitted bandwidth is varied with the help of the digital filter used in the transmission. The symbol rate and the modulation format are kept constant to 1 GBd and QPSK. A relatively homogeneous difference between the performance of the multichannel and of the single channel transmission of around 3 % is observed, which means that inter-channel interference negatively affect the quality of the link. This effect can be also observed in Fig. 16, which shows the EVM in dependency of the frequency spacing between the two transmitted channels. When the gap is small, in the order of magnitude of around 250 MHz the EVM of each channel reaches 8 %. By increasing the spacing to 750 MHz the performance improves by 1 %.

The successful transmission of aggregated channels, compatible to the new IEEE standard, with such high data rates shows the potential of the presented wireless link for future high data rate applications. Furthermore, the used complex modulation format, 64-QAM, is another promising factor for reaching high data rates with terahertz communication links.

## VII. Conclusion

This paper reports on a 300 GHz superheterodyne system, that reaches a maximum data rate of 60 Gbps and can cover distances up to 10 m. Two possibilities of realizing the superheterodyne architecture are analyzed: with commercial, easily accessible mixers and with an AWG. A comparison to zero-IF configuration shows the advantages of the superheterodyne architecture. The EVM is improved for all modulation formats. The link shows compatibility to low-cost existing baseband solutions and to the new IEEE frequency standard for ultra-fast communication networks. Channel aggregation is proven feasible, by the successful transmission of complex modulated signals, 64-QAM. A channel data rate of 10.2 Gbps is reached. Although a redesign of the 300 GHz transmitter and receiver needs to be made, so that the circuits are particularly designed for superheterodyne configuration, with an IF frequency of 70 GHz this experiment validates the applicability of terahertz communication.

## Acknowledgment

This work has received funding from Horizon 2020, the European Union's Framework Programme for Research and Innovation, under grant agreement No. 814523. ThoR has also received funding from the National Institute of Information and Communications Technology in Japan (NICT). We express our gratitude to the colleagues at Fraunhofer Institute of Applied Solid-State Physics for MMIC manufacturing. We also thank the IEMN Nano-Microwave RF/MEMS characterization centre and the IEMN-IRCICA Telecom platform facilities.

## References

[1] G. Fettweis and S. Alamouti, "5g: Personal mobile internet beyond what cellular did to telephony," *IEEE Communications Magazine*, vol. 52, no. 2, pp. 140–145, February 2014.

[2] *IEEE Standard for High Data Rate Wireless Multi-Media Networks Amendment 2: 100 Gbps Wireless Switched Point-to-Point Physical Layer*, IEEE-SA Standards Board Std.

[3] V. K. Chinni, P. Latzel, M. Zégaoui, C. Coinon, X. Wallart, E. Peytavit, J. F. Lampin, K. Engenhardt, P. Szriftgiser, M. Zaknoune, and G. Ducournau, "Single-channel 100 Gbit/s transmission using III–V UTC-PDs for future IEEE 802.15.3d wireless links in the 300 GHz band," *Electronics Letters*, vol. 54, no. 10, pp. 638–640, 2018.

[4] S. Jia, X. Pang, O. Ozolins, X. Yu, H. Hu, J. Yu, P. Guan, F. D. Ros, S. Popov, G. Jacobsen, M. Galili, T. Morioka, D. Zibar, and L. K. Oxenløwe, "0.4 THz Photonic-Wireless Link with 106 Gbps Single Channel Bitrate," *Journal of Lightwave Technology*, vol. 36, no. 2, pp. 610–616, Jan 2018.

[5] S. Koenig, D. Lopez-Diaz, J. Antes, F. Boes, R. Henneberger, A. Leuther, A. Tessmann, R. Schmogrow, D. Hillerkuss, R. Palmer, T. Zwick, C. Koos, W. Freude, O. Ambacher, J. Leuthold, and I. Kallfass, "Wireless sub-THz Communication System with High Data Rate Enabled by RF Photonics and Active MMIC Technology," in *2014 IEEE Photonics Conference*, Oct 2014, pp. 414–415.

[6] C. Castro, S. Nellen, R. Elschner, I. Sackey, R. Emmerich, T. Merkle, B. Globisch, D. de Felipe, and C. Schubert, "32 gbd 16qam wireless transmission in the 300 ghz band using a pin diode for thz upconversion," in *2019 Optical Fiber Communications Conference and Exhibition (OFC)*, March 2019, pp. 1–3.

[7] H. Hamada, T. Fujimura, I. Abdo, K. Okada, H. Song, H. Sugiyama, H. Matsuzaki, and H. Nosaka, "300-GHz 100 Gbps InP-HEMT Wireless Transceiver Using a 300-GHz Fundamental Mixer," in *2018 IEEE/MTT-S International Microwave Symposium - IMS*, June 2018, pp. 1480–1483.

[8] S. Hara, K. Takano, K. Katayama, R. Dong, S. Lee, I. Watanabe, N. Sekine, A. Kasamatsu, T. Yoshida, S. Amakawa, and M. Fujishima, "300-GHz CMOS Transceiver for Terahertz Wireless Communication," in *2018 Asia-Pacific Microwave Conference (APMC)*, Nov 2018, pp. 429–431.

[9] S. Lee, R. Dong, T. Yoshida, S. Amakawa, S. Hara, A. Kasamatsu, J. Sato, and M. Fujishima, "9.5 an 80gb/s 300ghz-band single-chip cmos transceiver," in *2019 IEEE International Solid- State Circuits Conference - (ISSCC)*, Feb 2019, pp. 170–172.

[10] P. Rodríguez-Vázquez, J. Grzyb, B. Heinemann, and U. R. Pfeiffer, "A 16-QAM 100-Gbps 1-m Wireless link with an EVM of 17an SiGe technology," *IEEE Microwave and Wireless Components Letters*, vol. 29, no. 4, pp. 297–299, April 2019.

[11] P. Rodríguez-Vázquez, J. Grzyb, B. Heinemann, and U. R. Pfeiffer, "Performance Evaluation of a 32-QAM 1-Meter Wireless Link Operating at 220–260 GHz with a Data-Rate of 90 Gbps," in *2018 Asia-Pacific Microwave Conference (APMC)*, Nov 2018, pp. 723–725.

[12] F. Boes, T. Messinger, J. Antes, D. Meier, A. Tessmann, A. Inam, and I. Kallfass, "Ultra-broadband MMIC-based wireless link at 240 GHz enabled by 64GSpros DAC," in *2014 39th International Conference on Infrared, Millimeter, and Terahertz waves (IRMMW-THz)*, Sept 2014, pp. 1–2.

[13] I. Kallfass, B. Florian, M. Tobias, A. Jochen, I. Anns, L. Ulrich, T. Axel, and H. Ralf, "64 Gbps transmission over 850 m Fixed Wireless Link at 240 Ghz Carrier Frequency," *Journal of Infrared, Millimeter, and Terahertz Waves*, vol. 36, no. 2, pp. 221–233, 2015. [Online]. Available: http://dx.doi.org/10.1007/s10762-014-0140-6

[14] Tech. Rep. [Online]. Available: https://www.etsi.org/deliver/etsi_en/302200_302299/30221702/03.00.08_20/en_30221702v030008a.pdf

[15] I. Dan, S. Rey, T. Merkle, T. Kürner, and I. Kallfass, "Impact of modulation type and baud rate on a 300ghz fixed wireless link," in *2017 IEEE Radio and Wireless Symposium (RWS)*, Jan 2017, pp. 86–89.

[16] [Online]. Available: https://ww2.minicircuits.com/pdfs/ZX05-24MH+.pdf

[17] I. Kallfass, P. Harati, I. Dan, J. Antes, F. Boes, S. Rey, T. Merkle, S. Wagner, H. Massler, A. Tessmann, and A. Leuther, "Mmic chipset for 300 ghz indoor wireless communication," in *2015 IEEE International Conference on Microwaves, Communications, Antennas and Electronic Systems (COMCAS)*, Nov 2015, pp. 1–4.

[18] A. Leuther, A. Tessmann, H. Massler, R. Losch, M. Schlechtweg, M. Mikulla, and O. Ambacher, "35 nm metamorphic HEMT MMIC technology," in *Indium Phosphide and Related Materials, 2008. IPRM 2008. 20th International Conference on*, May 2008, pp. 1–4.

[19] A. Tessmann, A. Leuther, S. Wagner, H. Massler, M. Kuri, H. . Stulz, M. Zink, M. Riessle, and T. Merkle, "A 300 GHz low-noise amplifier S-MMIC for use in next-generation imaging and communication applications," in *2017 IEEE MTT-S International Microwave Symposium (IMS)*, June 2017, pp. 760–763.

[20] J. Chen, D. Kuylenstierna, S. E. Gunnarsson, Z. S. He, T. Eriksson, T. Swahn, and H. Zirath, "Influence of white lo noise on wideband communication," *IEEE Transactions on Microwave Theory and Techniques*, vol. 66, no. 7, pp. 3349–3359, July 2018.

[21] J. Antes and I. Kallfass, "Performance estimation for broadband multi-gigabit millimeter- and sub-millimeter-wave wireless communication links," *IEEE Transactions on Microwave Theory and Techniques*, vol. 63, no. 10, pp. 3288–3299, Oct 2015.

[22] R. Weber, A. Tessmann, M. Zink, M. Kuri, I. Kallfass, H. . Stulz, M. Riessle, H. Massler, T. Maier, A. Leuther, and M. Schlechtweg, "A w-band x12 frequency multiplier mmic in waveguide package using quartz and ceramic transitions," in *2011 IEEE Compound Semiconductor Integrated Circuit Symposium (CSICS)*, Oct 2011, pp. 1–4.

[23] A. Georgiadis, "Gain, phase imbalance, and phase noise effects on error vector magnitude," *IEEE Transactions on Vehicular Technology*, vol. 53, no. 2, pp. 443–449, March 2004.

[24] F. Chang, K. Onohara, and T. Mizuochi, "Forward error correction for 100 G transport networks," *IEEE Communications Magazine*, vol. 48, no. 3, pp. S48–S55, March 2010.

[25] R. . S. B. Divison, "Bit Error Ratio BER as a function of SNR," Rohde & Schwarz, Tech. Rep.

[26] A. R. I. Rishad Ahmed Shaik, Md. Shahriar Rahman, "On the Extended Relationship Among EVM, BER, and SNR as Performance Metrics," in *4th International Conference on Electrical and Computer Engineering ICECE*, 2006.


**Iulia Dan** received the B.Sc. and M.Sc. Degree in Electrical Engineering from the University of Stuttgart in 2012 and 2015, respectively. Currently, she is pursuing her Ph.D. as a research assistant with the Institute of Robust Power Semiconductor Systems at the University of Stuttgart, with a focus on 300 GHz transmit-receive systems for ultra-fast communication.

**Guillaume Ducournau** obtained the engineering degree from ESIGELEC, Rouen, France in 2002 and the M.Sc. degree at Rouen University. In 2002, he worked in Canada (Montréal) on the characterization of optical fiber Bragg gratings for core optical networks. In 2005, he obtained the PhD degree from Université de Rouen, France on fiber optic communication systems using DPSK/DQPSK modulation schemes. He was an Assistant Professor at the IEMN (Institute of Electronics, Microelectronics and Nanotechnology) / University of Lille 1 and Polytech'Lille Graduate School, in the THz Photonics group during 2007-2018. He is now full professor since 2018. G. Ducournau is the leader of the THz wireless communications activity at IEMN using optoelectronic THz photomixers, electronic receivers, THz instrumentation and mm-wave characterization. He is author or co-author of more than 130 publications in peer-reviewed international journals or peer reviewed conferences proceedings and holds 1 patent. He has worked on several ANR and European projects (ITN "MITEPHO" and STREP "ROOTHz"). G. Ducournau was the coordinator of the French ANR COM'TONIQ project (2014-2017) funded by ANR (INFRA 2013) dedicated to THz communications in the 300 GHz band. He actually coordinates the ERA-NET TERALINKS program in which the main goal is the achievement of THz system level demonstrators based on advanced technologies in the 220-320 GHz range, and the ANR/DFG TERASONIC project for the use of THz photonics technologies and electrical solid-state technologies towards a complete 300 GHz transmission system for 100 Gbps wireless links. He is also member of the ThoR project, an EU-Japan funded project for the development of km-range super-heterodyne THz transmission systems for the new IEEE 802.15.3d standard.

**Shintaro Hisatake** received his M.E. and Ph.D degrees in electrical engineering from Doshisha University, Kyoto, Japan in 2000 and 2003, respectively. From 2003 to 2017 he was an assistant professor at the Graduate School of Engineering Science, Osaka University, Osaka, Japan. Since April 2017, he has been an associate professor at Gifu University, Gifu, Japan, where his major fields of research are generation, manipulation, and detection of millimeter- and THz waves and their applications. In 2014, he received The Optics Prize for Excellent Papers 2013 from the Japan Society of Applied Physics, and the Osaka University Presidential Awards for Encouragement (2014, 2015). In 2016, he was awarded the Young Scientists' Prize of the Commendation for Science and Technology by the Minister of Education, Culture, Sports, Science and Technology, Japan.

**Pascal Szriftgiser** received in 1996 the Ph.D. degree (“quantum physics”) from University Paris VI, Laboratoire Kastler Brossel, Paris (France). He then joined laboratory PhLAM (Physique des Lasers Atomes et Molécules) as a CNRS Researcher. He is currently a Research Director, the leader of the Cold Atoms group and deputy director of laboratory PhLAM. His expertise spans from cold atoms physics, quantum chaos, nonlinear optics in optical fibers to coherent optical communications. He is coauthor of 68 publications in peer-reviewed journals.

**Ralf-Peter Braun** received his MS and PhD in Electrical Engineering from the Technical University Berlin, Germany, in 1985 and 1995, respectively. He has more than 30 years of research and industry experience on optical transmission systems and network architectures. After 14 years of research work at the Heinrich-Hertz-Institute, Berlin, Germany, he joined Deutsche Telekom in 1997. He is engaged in network architecture, technology, service, control, Terahertz communications, test networks, and standardization. He is a member of VDE, ITG, and IEEE802.3 working group.

**Ingmar Kallfass** received the Dipl.-Ing. degree in Electrical Engineering from University of Stuttgart in 2000, and the Dr.-Ing. degree from University of Ulm in 2005. In 2001, he worked as a visiting researcher at the National University of Ireland, Dublin. In 2002, he joined the department of Electron Devices and Circuits of University of Ulm as a teaching and research assistant. In 2005, he joined the Fraunhofer Institute for Applied Solid-State Physics. From 2009 to 2012, he was a professor at the Karlsruhe Institute of Technology. Since 2013, he holds the chair for Robust Power Semiconductor Systems at the University of Stuttgart, where his major fields of research are compound semiconductor based circuits and systems for power and microwave electronics.